

Fluorescence from the Highly Excited States and Vibrational Energy Relaxation in Directly Linked Porphyrin Arrays

Nam Woong Song, Hyun Sun Cho,† Min-Chul Yoon,† Sae Chae Jeoung, Naoya Yoshida,†† Atsuhiro Osuka,*,†† and Dongho Kim*,†

Laser Metrology Laboratory, Korea Research Institute of Standards and Science, Taejon 305-600, Korea

†Center for Ultrafast Optical Characteristics Control and Department of Chemistry, Yonsei University, Seoul 120-749, Korea

††Department of Chemistry, Graduate School of Science, Kyoto University, Kyoto 606-8502

(Received September 10, 2001)

The fluorescence decay profiles of zinc(II) 5,15-di-(3,5-di-*tert*-butylphenyl) porphyrin monomer (Z1) and its *meso*, *meso*-linked dimer (Z2), trimer (Z3) and tetramer (Z4) were investigated by using the fluorescence upconversion technique. Fluorescence from the S_2 state in Z1 was observed to decay with the time constant of 1.2 ps at 460 nm. Corresponding fluorescence rise due to the internal conversion from S_2 to S_1 states in Z1 was also observed at 635 nm with the time constant of 1.5 ps. The S_2 state lifetime of Z2 was largely reduced (90 fs) due to the participation of exciton-split Soret band as a ladder type deactivation channel. Fluorescence decay profile and time-resolved spectra in 530 – 600 nm region revealed that the intramolecular vibrational relaxation (IVR) rate is retarded as the excess vibrational energy decreases in the porphyrin arrays as well as in Z1. The IVR rate was increased from Z1 to Z2 probably due to the additional normal modes related with the inter-unit bond as an efficient internal bath. Furthermore it was observed that a bottleneck in the bath modes limits the increase of IVR rate with the increased number of internal modes in the arrays over Z2 molecule.

The intramolecular vibrational relaxation (IVR) is one of the primary molecular processes occurring immediately after photoexcitation. This process competes with ultrafast energy transfer between electronic states,[1] the configuration change of the surrounding solvent molecules,[2] and geometric changes such as photoisomerization and photodissociation so that the rate, pathways, and efficiencies of these processes largely depend on IVR process. Thus the detailed knowledge about IVR process is fundamental to elucidate various kinds of ultrafast phenomena. Much efforts have been devoted to deduce the rate constant and detailed mechanism of ultrafast vibrational relaxation by using time-resolved Raman spectroscopy,[3] femtosecond pump-probe method,[4] and fluorescence upconversion technique.[5] The dynamics of vibrational relaxation process largely depends on the nature of molecules. It is generally accepted that the typical time scale of IVR process is in the subpicosecond range.[6] Such a fast rate constant has been revealed through the progress in ultrafast laser spectroscopy that enables a direct time domain observation of excited state population. Among the various methods, fluorescence upconversion technique is one of the most powerful tools for studying the excited state dynamics through fluorescence detection devoid of any interference from the dark states.[7]

Meanwhile, a major source of inspiration for the design and synthesis of optical nanostructures comes from the light-harvesting antenna complexes of natural photosynthetic systems.[8] The antenna complexes are comprised of a large number of pigments that are arranged in a rigid three-dimensional matrix. The natural antenna complexes absorb light and funnel the resultant energy to the reaction centers by means of excited-state energy transfer processes. The versatile optical (absorption and emission), redox, and photochemical properties of the porphyrins make them ideally suited as components of nanostructures. Continuing efforts to realize the mimicry of solar energy harvesting complexes have enabled the design and synthesis of various types of covalently linked porphyrin arrays with the goal of applying these arrays to molecular photonic devices and artificial light-harvesting array systems.

Multi-porphyrin arrays have been constructed using several types of shorter linkers that are suitable for preparing linear or extended architectures via *meso* position attachment. In this regard, the directly linked porphyrin arrays could provide the prospects as artificial light harvesting arrays and molecular photonic wires since the unique photophysical aspect of these molecular arrays arising from substantial interchromophic electronic interactions fully mimic the biological light harvesting assemblies that facilitate ultrafast energy migration mediated by protein environment. Recently, there is a progress in synthesizing capabilities of porphyrin arrays in which porphyin pigments are directly connected together through *meso* positions without any linkers.[9] It was demonstrated that the spectral and electronic properties of pigments, and linkage structure have a strong influence on the overall photophysical properties of porphyrin oligomers.[10] Especially, there is a unique feature in the absorption spectra arising from strong excitonic interactions between the adjacent porphyrin units in the arrays.

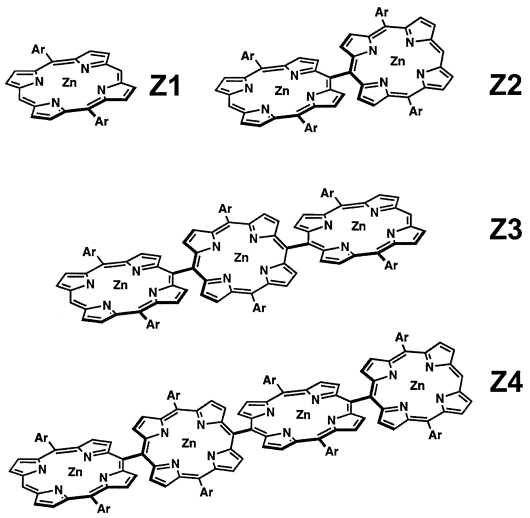

Scheme 1. Molecular structures of synthesized porphyrin monomer and arrays.

In the present work, we have investigated the ultrafast excited state dynamics such as internal conversion (IC) and vibrational energy redistribution through IVR process in directly linked Zn(II) porphyrin arrays (Scheme 1) by using the fluorescence upconversion technique. Systematically increased array compounds in the subunits such as monomer (Z1), dimer (Z2), trimer (Z3) and tetramer (Z4) were synthesized and studied for the elucidation of ultrafast fluorescence dynamics change with the increased number of electronic states and vibrational modes.

Experimental

Zinc(II) 5,15-di-(3,5-di-*tert*-butylphenyl) porphyrin monomer (Z1), and its *meso*, *meso*-linked porphyrin dimer (Z2), trimer (Z3), and tetramer (Z4) were synthesized.[9] (Scheme 1) The spectroscopic grade tetrahydrofuran (THF) and toluene were used as solvents. The absorption spectra of prophyrins in THF were recorded by using a Varian Cary 3 spectrophotometer and fluorescence measurement were made on a scanning SLM-AMINCO 4800 fluorometer. Toluene was used as the solvent for both steady-state and time resolved fluorescence measurements.

The details for the fluorescence upconversion measurement can be found elsewhere[7] and a brief description will be given here. The light source is a mode-locked Ti:sapphire laser (Coherent, MIRA) pumped by a intra-cavity frequency doubled CW Nd:YAG laser (Coherent, Verdi). The oscillator output pulse train is 550 mW at 800 nm with typical pulse duration of 120 fs observed by SHG (second harmonic generation) autocorrelation trace. The second harmonic pulse (λ = 400 nm, 90 mW) is generated by using a β-BBO (1 mm thick) crystal. The residual fundamental pulse after the dichroic mirror (CVI) is used as a gate pulse for the upconversion of fluorescence. The time interval between the fluorescence light and gate pulse is controlled by a delay stage equipped with a corner cube gold retro-reflector (Coherent, 2″ diameter) with travelling the gate pulse. The excitation pulse power is controlled by using a variable neutral density filter (Sigma, 1 mm thick) and then focussed onto the sample glass cell (flow type, 1 mm thick) by using a 5 cm focal length aluminum coated parabolic mirror (Coherent). Fluorescence light is collected and focussed onto the β-BBO (1 mm thick, type-I) crystal for the upconversion by using an aluminum coated parabolic mirror (Coherent, 5 and 20 cm in focal lengths). A cutoff filter (Schott Glass Filter Co., GG475, 3 mm thick) is placed between the collimating and focussing mirrors to remove the transmitted pump pulse. The sample was circulated to the flow cell to minimize the signal change by sample degradation and thermal lensing effect. Upconverted signal from the sum frequency generation crystal is focussed on the entrance slit of the 320 mm focal length monochromator (HR320, Jobin-Yvon) after passing through the UV bandpass filter (Schott Glass Filter Co., UG11). The spectral resolution in the UV region was kept to be 5 nm through all the experiments. The signal is detected by a head-on type photomultiplier tube (Hamamatsu, model 3235) with a gated photon counter (Stanford Research Systems, SR400). The gated photon counter is interfaced with a personal computer which controls the delay stage. The time resolution of the upconversion measurements is ~310 fs as estimated from the full width at half maximum of the cross-correlation trace between the excitation and the gate pulses.

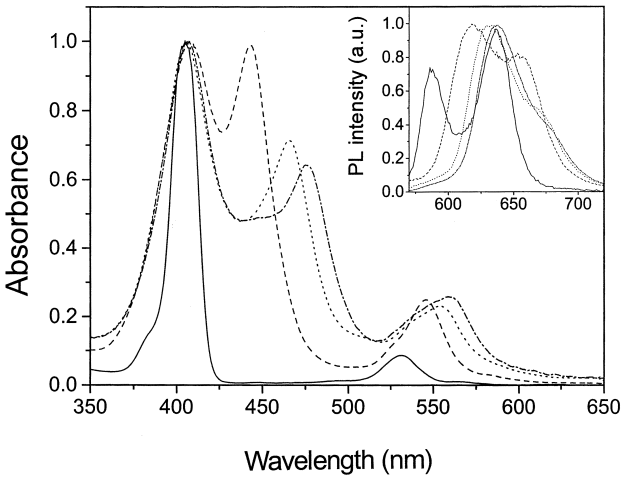

Fig. 1. Absorption and fluorescence (inset) spectra of Z1 (—), Z2 (---), Z3 (····) and Z4 (-·-·-) in THF.

Results and Discussion

Absorption and emission spectra of Z1, Z2, Z3 and Z4 are shown in Fig. 1. The absorption spectra denote interesting systematic changes in the Soret bands with an increase in the number of porphyrin moieties. While the Soret band of Z1 exhibits a single absorption maximum at 411 nm, that of Z2 is split into two bands with absorption peaks at 415 and 457 nm. In the cases of Z3 and Z4, the splitting of the Soret band becomes more significant, exhibiting two Soret bands at 413 and 472 nm in Z3 and at 413 and 485 nm in Z4, respectively. These systematic changes are attributable to the exciton coupling between the adjacent porphyrin moieties.[10] On the other hand, the Q-band absorption was not much affected by the addition of porphyrin moieties. There was no distinct excitonic band splitting in the Q-band absorption of Z2, Z3, and Z4 arrays due to a low oscillator strength of Q-band. A slight redshift of the absorption maximum was observed with an increase in the number of porphyrin moieties, indicating that π-electron delocalization throughout the arrays is negligible due

to the orthogonal arrangement between the neighboring porphyrin units. In the absorption spectrum of Z1, the vibronic structure was observed with the 0–0 band transition intensity being very weak ($\lambda_{0\text{–}0,max} \sim 567$ nm). Higher vibronic absorption band at $\sim$1180 cm^{-1} above the 0–0 band was observed with about seven times higher intensity of the 0–0 band. Such an absorption profile can be considered as due to the structural change in the S_1 state compared with the S_0 state which results in the decrease of 0–0 and increase of 1–0 transition probabilities or Franck–Condon factors. A similar behavior was also observed in the absorption spectra of Z2, Z3 and Z4 with further reduced relative intensity of 0–0 transition band. The fluorescence spectra of Z1 exhibit vibronic emission bands at 587 and 637 nm (Inset of Fig. 1) with a moderate Stokes shift of $\sim$825 cm^{-1}. As the number of porphyrin ring units increases, the emission bands of the arrays are red-shifted with a decrease in the relative intensity of the low-energy side.

According to the four-orbital model, the low-lying (π, π^*) excited states of porphyrins can be described in terms of the transitions between two highest occupied molecular orbitals (HOMO's), $a_{2u}(\pi)$ and $a_{1u}(\pi)$, and two degenerate lowest unoccupied molecular orbitals (LUMO's), $e_g(\pi^*)$. For the porphyrin ring, the lowest singlet excited configurations, $a_{2u}(\pi)$, $e_g(\pi^*)$ and $a_{1u}(\pi)$,$e_g(\pi^*)$, are nearly degenerate, and as a consequence there is a strong electronic interaction between them. The resulting resonance yields the relatively weak visible Q-band, in which the transition dipoles of the two configurations nearly cancel, and the intense Soret band, in which the transition dipoles of the two configurations add. Thus, in reality the Q band of porphyrin monomer borrows its intensity from the B band through vibronic coupling. In the cases of porphyrin arrays, the existence of exciton-split B bands between unshifted monomeric B bands and Q bands reduces the energy difference between B and Q bands, which results in an increase in intensity borrowing of Q bands from B bands. Therefore the intensities of Q bands of porphyrin arrays increase in parallel with an increase in the exciton splitting as the number of porphyrin units increases in the porphyrin arrays.

Primarily we observed the ultrafast decay dynamics of Z1 fluorescence at various wavelengths as shown in Fig. 2. When

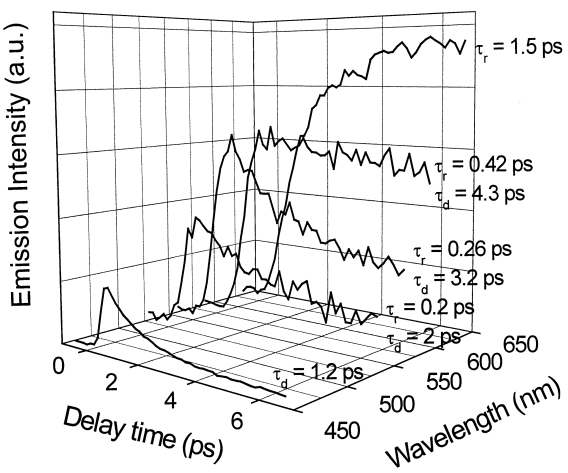

Fig. 2. Temporal profiles of Z1 fluorescence at various probe wavelengths.

we excited Z1 with 400 nm laser pulses, the fluorescence decay profile at 460 nm exhibited a single exponential decay with the time constant of 1.2 ps (Fig. 2). The probe wavelength dependence of fluorescence decay profiles of Z1 in 530 – 600 nm region shows both rise and decay components with the increase of both time constants as the probe wavelength increases. When the probe wavelength was 640 nm, no decay profile but only the rise with the time constant of 1.5 ps was observed in the short time window (10 ps).

The fast single exponential decay at 460 nm is attributable to the radiative decay of $S_2 \rightarrow S_0$ transition. This unusual phenomenon which violates the well-known Kasha's rule[11] has often been observed in the fluorescence of molecules such as azulene,[12] *s*-indacene[13] and metalloporphyrins[14] in which the S_2–S_1 energy gap is relatively large so that the internal conversion between the S_2 and S_1 states is relatively slow. In case of metalloporphyrins, there is a relatively large energy separation between the S_2 and S_1 excited states which appear as Q and B bands in UV-visible region. Furthermore, these two states are considered as a 50–50 admixture of two common excited electronic configurations $^1(a_{1u},e_g)$ and $^1(a_{2u},e_g)$ in accidental degeneracy, and the energy surfaces of the S_1 and S_2 excited states are almost parallel. This definitely retards the $S_2 \rightarrow S_1$ intramolecular electronic internal conversion processes.[15] It is already established that the S_2 states of 5,10,15,20-tetraphenyl and 5,15-diphenyl zinc(II) porphyrin analogs are relatively long-lived with lifetimes of 1 – 2 ps.[14b–c,15] Since Z1 compound is zinc(II) 5,15-di-(3,5-di-*tert*-butylphenyl) porphyrin, the 1.2 ps lifetime of the S_2 state seems to be quite reasonable. Moreover, a similar time constant (1.5 ps) of rise was observed in the Z1 fluorescence at 635 nm (Fig. 2). Since the intramolecular vibrational redistribution is known to take place in a few hundreds of femtoseconds for large molecules,[6] the fluorescence rise at 635 nm might be mainly due to the internal conversion process between the S_2 and S_1 electronic states. A little difference in the $S_2 \rightarrow S_0$ decay time (1.2 ps, 460 nm probe) and $S_1 \rightarrow S_0$ rise time (1.5 ps, 635 nm probe) can be understood as due to the partial contribution of the IVR process in the S_1 manifolds of Z1. This 1.5 ps rise time does not seem to be due to the result of vibrational cooling which occurs via solvent–solute interaction since this process in the S_1 states of porphyrin monomers occurs on the time scale of 10 – 20 ps.[16]

The change of fluorescence decay profiles in Z1 at various probe wavelengths in 530 – 600 nm region (Fig. 2) indicates the existence of the vibrational energy redistribution through IVR process in the S_1 manifolds. We can observe both rise and decay time constants as the probe wavelength increases. The decrease of the decay rate along with the increase of probe wavelength can be understood by the fact that the IVR process is retarded as the excess energy in a specific vibrational mode decreases.[17] The shorter rise time than the decay time of the S_2 fluorescence is ascribable to the fast decay time of vibronic states ($\tau_d < 1.2$ ps). The rise and decay time constants appear as to be exchanged value when the decay time is shorter than the rise time in a consecutive decay mechanism. Observation of relatively slow decay time (3.5 ps) with a fast rise time ($\sim$250 fs) is ascribable to the contribution of fluorescence from both the highly excited ($\tau_d \sim 0.25$ ps) and lower excited

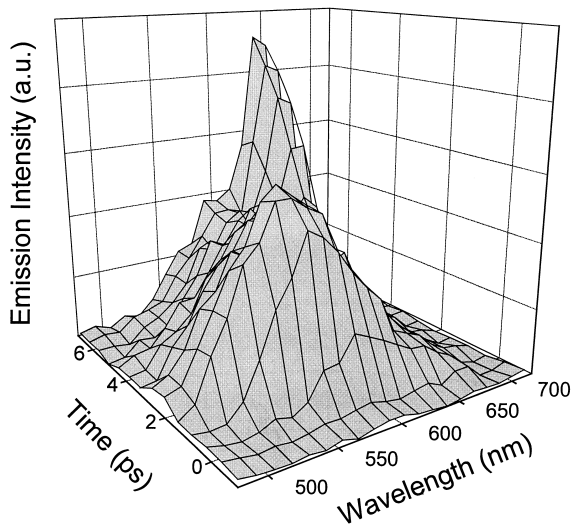

Fig. 3. Time resolved fluorescence spectra of Z1 at various delay times.

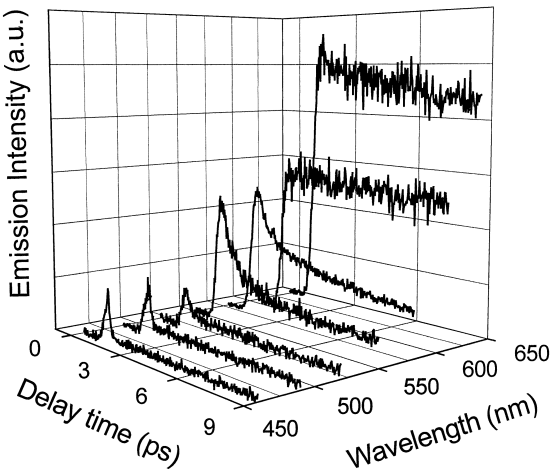

Fig. 4. Temporal profiles of Z2 fluorescence at various probe wavelengths.

(τ_d = 3.5 ps) vibrational states since the spectral resolution for the detection of upconverted light was not so narrow.

To observe the time evolution of the ultrafast fluorescence dynamics, we have measured the time-resolved fluorescence spectra of Z1 at various delay times as shown in Fig. 3. The emission spectrum exhibits the maximum value around 560 nm at early stage, and the band decays rapidly with ~2 ps decay time constant to result in the emission maximum showing at longer wavelengths as the time delay is increased. The emission maxima appears at ~590 nm (shoulder) and ~635 nm which correspond to the two emission maxima in the steady-state fluorescence. The fluorescence transient at ~1 ps having maximum around 560 nm, where the emission intensity is negligible in the steady-state fluorescence spectrum, is probably due to the emission from the excited vibrational states in the S_1 manifolds. It is considered that the retardation of vibrational relaxation decay rate and the increase of Franck–Condon factors of vibronic transitions result in the transient maximum of emission intensity at the excited vibrational states in the S_1 manifolds.[5c,18] The rate equation corresponding to the population change of a vibrational state can be described as follows;

$$\mathrm{d}N^{v}(S_1)/\mathrm{d}t = k_{IC}\,N(S_2) + k_d(v')N^{v'}(S_1) - k_d(v)\,N^{v}(S_1) - k_r(v)\,N^{v}(S_1) \quad (1)$$

where $N^{v'}(S_1)$, $N^{v}(S_1)$, and $N(S_2)$ denote the population of $S_1^{v'}$, S_1^{v} and S_2 states, respectively, in which the superscripts v′ and v represent the vibrationally excited states (v′>v) in the electronically excited S_1 manifolds. k_{IC} corresponds to the internal conversion rate between the S_2 and S_1 electronic states, and $k_d(v')$ and $k_d(v)$ indicate the IVR rates at the $S_1^{v'}$ and S_1^{v} states, respectively. k_r represents the radiative decay rate from the S_1^{v} state to the vibronic states in the S_0 state, which largely depends on the Franck–Condon factor of corresponding transition. The fluorescence intensity (I_F^{v}) of an individual vibronic state (S_1^{v}) might be proportional to the radiative transition rate according to the following equation.

$$I_F^{v} \propto (k_r/[k_d(v) + k_r]) \quad (2)$$

At higher vibrational states, the rate of IVR process (k_d) is expected to be very fast, while the radiative decay rate (k_r) would be slow due to the poor Franck–Condon factors. Thus the emission intensity at highly excited states might be very low. However, as the vibrational quanta in specific — Franck–Condon active — modes decreases, the IVR process is retarded as shown in Fig. 2. On the other hand, the radiative decay rate tends to increase due to the favored Franck–Condon transition. This opposite trend of IVR rate and Franck–Condon factor result in a transient maximum corresponding to the transition energy close to the $S_1(v = 1) \rightarrow S_0(v = 0)$ transition. It can be observed from the absorption spectrum of Z1 that the $S_0(v = 0) \rightarrow S_1(v = 1)$ is the most favorable vibronic transition.

Fluorescence decay profiles of Z2 excited at 400 nm were observed at various wavelengths as shown in Fig. 4. Large differences between the dimer (Z2) and monomer (Z1) fluorescence temporal profiles were found in the time constants for the decay at 460 nm and rise at 650 nm. As shown in Fig. 4, the decay time of Z2 fluorescence at 460 nm (~90 fs) and the rise time at 650 nm (~300 fs) was much shorter than those in Z1 (1.2 and 1.5 ps, respectively). Since the fluorescence at 460 nm in Z1 is considered as due to the $S_2 \rightarrow S_0$ transition, the dramatic change of the 460 nm decay time means that the S_2 state lifetime is largely reduced by the linkage of porphyrin moieties. The decrease in the S_2 state lifetime is attributable to the generation of excitonic split band between the Soret and Q-bands, which provides a "ladder" for sequential relaxations for internal conversion between the S_2 and S_1 states.[10] According to the energy gap law,[19] the internal conversion rate is given as

$$k_{IC} \sim 10^{13}\exp(-\alpha\Delta E) \quad (3)$$

with α and ΔE being the proportionality constant and the energy gap between the zero vibrational states in two electronic states, respectively. Thus the internal conversion rate in dimer (Z2) might be much increased along with the large decrease in ΔE due to the addition of ladder state between the Soret and Q-bands. This behavior was also observed in the fluorescence decay profiles of Z3 and Z4 (Fig. 5 and Table 1). The internal

Table 1. Summary of Excited State Dynamics in the Porphyrin Arrays

	τ_1 (460 nm, decay)[a)]	τ_2 (560 nm, decay)	τ_3 (650 nm, rise)	τ_4 (S_1 lifetime)[c)]
Z1	1.2 ps	2 ps	1.5 ps	2.57 ns
Z2	90 fs	840 fs	300 fs	1.93 ns
Z3	Not observed[b)]	750 fs	500 fs	1.58 ns
Z4	Not observed[b)]	830 fs	700 fs	0.92 ns

a) $S_2 \rightarrow S_0$ transition. b) very week due to the re-absorption of fluorescence by the sample. c) measured by other experiment (TCSPC).[10]

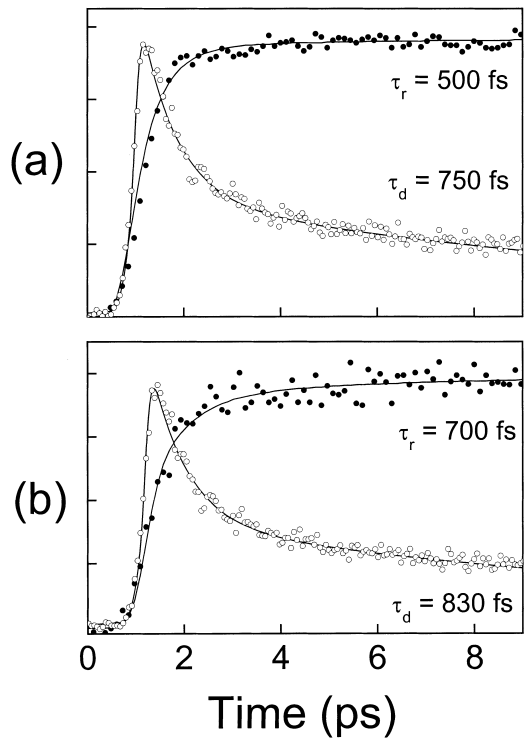

Fig. 5. Temporal profiles of fluorescence decay (a) Z3 at 560 and 660 nm, and (b) Z4 at 560 and 640 nm. The dots and lines represent the experimental data and fitted results, respectively.

conversion rate between the S_2 and S_1 states estimated from the rise time of long wavelength fluorescence was observed to follow the energy gap law very well.[10]

The ultrafast fluorescence dynamics of Z2 observed in the wavelength range between 530 and 600 nm exhibited another fast decay dynamics corresponding to the time constant of ~800 fs at 560 nm. This decay can be considered as due to the IVR process which was also observed in the temporal profile of Z1 fluorescence with the decay time constant of ~2 ps. The IVR rate is known to depend largely on the molecular geometry. For large molecules ($N > 30$), it is generally accepted that the IVR time constant is usually several hundreds femtoseconds.[6] However, it is also reported that relatively slow IVR rate (a few ps) can be observed even in large molecules depending on the molecular structure.[20] As the number of atoms in Z1 is 105, it is thought that the increased number of atoms in Z2 does not largely affect the IVR rate. Rather the newly formed normal modes related with the inter-unit bond seems to play an important role in the increase of IVR rate from Z1 to Z2. As a consequence, there was no distinct increase in the intramolecular vibrational redistribution rate when we observed the decay profiles of longer array molecules (Z3 and Z4). The decay profiles of Z2, Z3 and Z4 observed at 560 nm exhibited almost the same feature with the time constant of around 800 fs (Fig. 5 and Table 1). It is thought that the increased number of internal bath modes does not largely affect the IVR rate in the porphyrin arrays. Rather, additional normal modes related with the inter-unit bond are likely to be more responsible for the increased IVR rate. We can also observe that the IVR time constant is limited to be ~800 fs with the increased number of atoms in the porphyrin arrays. In the relaxation process of highly vibrationally excited states, a large part of excess energy is transferred from the Franck-Condon active high frequency modes to energy acceptors (bath modes) in the time range of femto- to subpicoseconds. At higher vibrationally excited states with excess energy over ~5000 cm^{-1}, the high frequency vibrations (1000 – 2000 cm^{-1}) in which one vibrational period is few tens of femtoseconds can participate as bath modes. The inclusion of high frequency vibrations in bath modes will result in the fast vibrational relaxation within few hundreds of femtoseconds since the rapid vibration of bath modes might give rise to fast and efficient energy relaxation. As the excess vibrational energy decreases, however, the high frequency vibrational modes can no longer play a role as bath modes because the energy available in the excited vibrational modes are comparable to or lower than the high frequency modes. In the energy region with excess energy below 3000 cm^{-1}, the medium (200 – 800 cm^{-1}) or low (< 200 cm^{-1}) frequency vibrational modes are expected to act as the major bath modes. As a result, the IVR rate becomes slow with the longer vibrational periods of bath modes if we assume that the IVR process occurs mainly through the momentum transfer. The vibrational excess energy for the 560 nm fluorescence in the porphyrin arrays (Z2, Z3 and Z4) corresponds to 1500 – 2500 cm^{-1}. It is expected that low frequency vibrational modes play a major role as bath modes for IVR process in this energy range. If we consider the average frequency of the bath oscillator to be 100 cm^{-1}, the time constant of 800 fs corresponds to 2.5 vibrational period. The similarity in the decay rate constants of 560 nm fluorescence in the porphyrin arrays (Z2, Z3 and Z4) can be explained in view of the bottleneck in the vibrational relaxation due to the slow vibrational period of bath modes in low excess energy region. Although the increase in the number of bath modes increases the probability of intramolecular vibrational energy transfer, a major contribution of low frequency vibrations to bath modes results in the bottleneck due to the slow motion of bath in low energy region.

When we reconstructed the time-resolved spectra from the

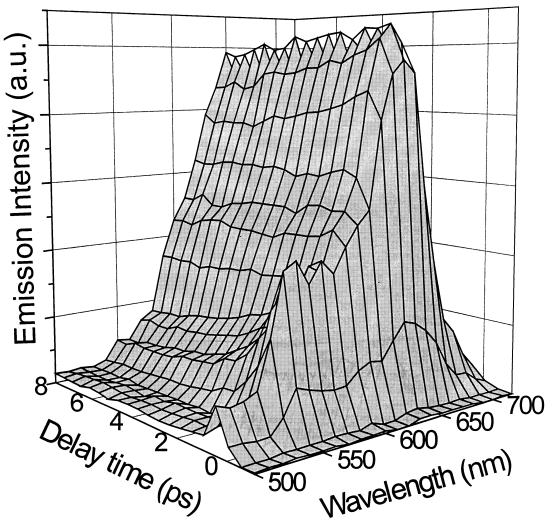

Fig. 6. Time resolved fluorescence spectra of Z2 at various delay times (Reconstructed from Fig. 4).

decay profiles of Z2 fluorescence at various wavelengths, we could observe a fast decaying shoulder in the energy region over 0–0 band transition as shown in Fig. 6. The fast decaying shoulder with the time constant of ~800 fs in the time resolved fluorescence spectra is attributable to the retardation of vibrational energy relaxation rate and favored Franck–Condon factor as in the time-resolved fluorescence spectrum of Z1. Since the rise time of Z2 fluorescence near 0–0 band transition was very short, we could not observe the spectral moving of the time-resolved fluorescence spectra, rather the spectral line narrowing due to the IVR process was observed. It is suggested that the IVR process proceeds in roughly two steps.[17] The optically pumped molecules in the highly excited vibrational levels of a specific vibrational mode, which is Franck–Condon active, relax very rapidly to the lower vibrational state in femto- to subpicosecond time range. Then slower relaxation occurs in longer time scale to achieve an intramolecular thermal equilibrium. It is also generally known that even in a large molecule, there is a bottleneck state in the IVR process in solution.[6b] Since the number of internal modes in Z2 is very large, the decay rate even at the bottleneck state is fast enough to be subpicosecond but slow to reveal the fluorescence at these states based on the favored radiative transition probabilities or Franck–Condon factors. The time-resolved spectra of Z3 and Z4 molecules are expected to be almost the same as that of Z2 considering the temporal profiles of the fluorescence decay. This process is not thought as due to the result of solvation dynamics, i.e. solvent reorientation motion relative to solute, since the emission energy is higher than that of 0–0 band absorption. The dynamic energy range for the Stokes shift due to the solvent reorientation lies below the 0–0 transition energy.[21]

Conclusion

We have measured the fluorescence decay profiles of the zinc(II) 5,15-di-(3,5-di-*tert*-butylphenyl)porphyrin monomer (Z1) and its *meso*, *meso*-linked dimer (Z2), trimer (Z3) and tetramer (Z4) by using the fluorescence upconversion technique. Fluorescence decay with 1.2 ps time constant from the S_2 state in Z1 was observed at 460 nm. Corresponding fluorescence rise due to the internal conversion between S_2 and S_1 state in Z1 was also observed at 635 nm with the time constant of 1.5 ps. The S_2 state lifetime of Z2 was largely reduced (90 fs) due to the participation of exciton split band as a ladder type deactivation channel. Fluorescence decay profiles and time-resolved spectra between 530 – 600 nm revealed that the intramolecular vibrational relaxation (IVR) rate is retarded as the excess vibrational energy decreases in the porphyrin arrays as well as in Z1. The IVR rate was increased from Z1 to Z2 probably due to additional normal modes related with the inter-unit bond as an efficient internal bath. Furthermore it is observed that a bottleneck in the bath modes limits the further increase of IVR rate with the increased number of internal modes over Z2 array molecule.

This work has been financially supported by the National Creative Research Initiatives of the Ministry of Science & Technology of Korea (DK). The work at Kyoto was supported by Grant-in-Aids for Scientific Research from the Ministry of Education, Science, Sports and Culture and by CREST (Core Research for Evolutional Science and Technology) of Japan Science and Technology Corporation (JST).

References

1 a) N. A. van Dantzig, D. H. Levy, C. Vigo, and P. Piotrowiak, *J. Chem. Phys.*, **103**, 4894 (1995). b) K. Wynne, S. M. LeCours, C. Galli, M. J. Therien, and R. M. Hochstrasser, *J. Am. Chem. Soc.*, **117**, 3749 (1995).

2 a) W. Humbs, E. van Veldhoven, H. Zhang, and M. Glasbeek, *Chem. Phys. Lett.*, **304**, 10 (1999). b) J. Watanabe, H. Takahashi, and J. Nakahara, *Chem. Phys. Lett.*, **213**, 351 (1993).

3 a) R. Leonhardt, W. Holzapfel, W. Zinth, and W. Kaiser, *Chem. Phys. Lett.*, **133**, 373 (1987). b) S. Ruhman, B. Kohler, A. G. Joly, and K. A. Nelson, *IEEE J. Quantum Electron.*, **24**, 460 (1988). c) D. McMorrow, W. T. Lotshaw, and G. A. Kenney-Wallace, *IEEE J. Quantum Electron.*, **24**, 443 (1998). d) W. Zinth, R. Leonhardt, W. Holzapfel, and W. Kaiser, *IEEE J. Quantum Electron.*, **24**, 455 (1998).

4 a) J. Z. Zhang, M. A. Kreger, Q.-S. Hu, D. Vitharana, L. Pu, P. J. Brock, and J. C. Scott, *J. Chem. Phys.*, **106**, 3710 (1997). b) W. Wolfseder, L. Seidner, W. Domoke, G. Stock, M. Seel, S. Engleitner, and W. Zinth, *Chem. Phys.*, **233**, 323 (1998). c) X. Weng, Y. Kosoulas, P. M. Fauchet, J. A. Osaheni, and S. A. Jenekhe, *Phys. Rev. B*, **51**, 6838 (1995).

5 a) T. J. Kang, K. Ohta, K. Tominaga, and K. Yoshihara, *Chem. Phys. Lett.*, **287**, 29 (1998). b) G. Park and T. J. Kang, *Bull. Korean Chem. Soc.*, **19**, 799 (1998). c) N. Mataga, Y. Shibata, H. Chosrowjan, N. Yoshida, and A. Osuka, *J. Phys. Chem.*, **2000** in press.

6 a) T. Elsaesser and W. Kaiser, *Annu. Rev. Phys. Chem.*, **42**, 83 (1991). b) J. C. Owrutsky, D. Raffery, and R. M. Hochstrasser, *Annu. Rev. Phys. Chem.*, **45**, 519 (1994). c) A. Tokmakoff, D. Zimdars, R. S. Urldahl, R. S. Francis, A. S. Kwok, and M. D. Fayer, *J. Phys. Chem.*, **99**, 13310 (1995).

7 a) L. A. Halliday and M. R. Topp, *Chem Phys. Lett.*, **71**, 440 (1977). b) J. Shah, *IEEE J. Quantum Electron.*, **24**, 276 (1988). c) M. A. Kahlow, W. Jarzeba, T. P. BuBruil, and P. F. Barbara, *Rev. Sci. Inst.*, **59**, 1098 (1988).

8 a) M. Gouterman, D. Holten, and S. Lieberman, *Chem, Phys*., **25**, 139 (1977). b) C. K. Chang, *J. Heterocycl. Chem*., **14**, 1285 (1977). c) K. Ichimura, *Chem. Lett*., **1977**, 641. d) N. E. Kagan, D. Mauzerall, and R. B. Merrifield, *J. Am. Chem. Soc*., **99**, 5484 (1977). e) J. P. Collman, J. W. Prodolliet, and C. R. Leidner, *J. Am. Chem. Soc*., **108**, 2916 (1986). f) J. P. Collman, A. Q. Chong, G. B. Jameson, R. T. Oakley, E. Rose, E. R. Schmittou, and J. A. Ibers, *J. Am. Chem. Soc*., **103**, 516 (1981). g) S. Konishin, M. Hoshino, and M. Imamura, *J. Phys. Chem*., **86**, 4888 (1982). h) R. L. Brookfield, H. Ellul, and A. Harriman, *J. Chem. Soc., Faraday Trans.2*, **81**, 1837 (1985). i) K. M. Kadish, G. Moninot, Y. Hu, D. Dubois, A. Ibnlfassi, J.-M. Barbe, and R. Guilard, *J. Am. Chem. Soc*., **115**, 8153 (1993). j) Y. Kaizu, H. Maekawa, and H. Kobayashi, *J. Phys. Chem*., **90**, 4234 (1986).

9 a) A. Osuka and H. Shimidzu, *Angew. Chem., Int. Ed. Engl*., **36**, 135 (1997). b) R. G. Khoury, L. Jaquinod, and K. M. Smith, *Chem. Commun*., **1997**, 1057. c) T. Ogawa, Y. Nishimoto, N. Yoshida, N. Ono, and A. Osuka, *Chem. Commun*., **1998**, 337.

10 a) H. S. Cho, N. W. Song, Y. H. Kim, S. C. Jeoung, S. J. Hahn, D. Kim, S. K. Kim, N. Yoshida, and A. Osuka, *J. Phys. Chem. A*, **104**, 3287 (2000). b) N. Aratani, A. Osuka, D. Kim, Y. H. Kim, and D. H. Jeong, *Angew. Chem*., **39**, 1458 (2000). c) Y. H. Kim, D. H. Jeong, D. Kim, S. C. Jeong, H. S. Cho, S. K. Kim, N. Aratani, and A. Osuka, *J. Am. Chem. Soc*., **123**, 76 (2001).

11 M. Kasha, *Discuss. Faraday Soc*., **9**, 14 (1950).

12 a) M. Beer and H. C. Longuet-Higgins, *J. Chem. Phys*., **23**, 1390 (1955). b) G. Viswath and M. Kasha, *J. Chem. Phys*., **24**, 757 (1956). c) J. B. Birks, *Chem. Phys. Lett*., **17**, 370 (1972).

13 R. Klann, R. J. F. Bäuerle, Laermer, T. Elsaesser, M. Nieraeyer, and W. Lüttke, *Chem. Phys. Lett*., **169**, 172 (1990).

14 a) L. Bajema, M. Gouterman, and C. B. Rose, *J. Mol. Spectrosc*. **39**, 421 (1971). b) H. Chosrowjan, S. Tanigichi, T. Okada, S. Takagi, T. Arai, and K. Tokumaru, *Chem. Phys. Lett*., **242**, 644 (1995). c) G. G. Gurzadyan, T.-H. Tran-Thi, and T. Gustavsson, *J. Chem. Phys*., **108**, 385 (1998).

15 H. Kobayashi and Y. Kaizu, "Porphyrins: Excited States and Dynamics" ed by M. Gouterman, P. Rentzepis, and K. D. Straub, American Chemical Society Symposium Series 321, American Chemical Society, Washington (1986), P. 105.

16 a) H. S. Eom, S. C. Jeoung, D. Kim, J.-H. Ha, and Y.-R. Kim, *J. Phys. Chem. A*, **101**, 3601 (1997). b) J. Rodriguez, C. Kirmaier, and D. Holten, *J. Chem. Phys*., **94**, 6020 (1991). c) J. W. Petrich, J. L. Martin, D. Houde, C. Poyart, and A. Orszag, *Biochemistry*, **26**, 7914 (1987). d) J. W. Petrich, C. Poyart, and J. L. Martin, *Biochemistry*, **27**, 4049 (1988). e) E. R. Henry, W. A. Eaton, and R. M. Hochstrasser, *Proc. Natl. Acad. Sci. U.S.A*., **83**, 8982 (1986). f) R. G. Alden, M. D. Chavez, M. R. Ondrias, S. H. Courtney, and J. M. Friedman, *J. Am. Chem. Soc*., **112**, 3241 (1990).

17 a) T. Dahinten, J. Baier, and A. Seilmeier, *Chem. Phys*. **232**, 239 (1998). b) T. Nakabayashi, H. Okamoto, and M. Tasumi, *J. Phys. Chem. A*, **102**, 9686 (1998).

18 a) B. Kopainsky and W. Kaiser, *Chem. Phys. Lett*., **66**, 39 (1979). b) S. Akimoto, T. Yamazaki, I. Yamazaki, and A. Osuka, *Chem. Phys. Lett*., **309**, 177 (1999).

19 W. Siebrand, *J. Chem. Phys*., **46**, 440 (1967).

20 a) S. J. Doig, P. J. Reid, and R. A. Mathies, *J. Phys. Chem*., **95**, 6372 (1991). b) M. C. Schneebeck, L. E. Vigil, and M. R. Ondarias, *Chem. Phys. Lett*., **215**, 251 (1993). c) S. G. Kruglik, Y. Mizutani, and T. Kitagawa, *Chem. Phys. Lett*., **266**, 283 (1977).

21 E. R. Middelhoek, H. Zhang, J. W. Verhoeven, and M. Glasbeek, *Chem. Phys. Lett*., **267**, 525 (1997).